Available online at www.sciencedirect.com
SCIENCE DIRECT®
Leukemia Research 29 (2005) 943–949
Leukemia Research
www.elsevier.com/locate/leukres

Retroviral expression screening of oncogenes in natural killer cell leukemia

Young Lim Choi [a, b], Ryozo Moriuchi [c], Mitsujiro Osawa [d], Atsushi Iwama [d], Hideki Makishima [e], Tomoaki Wada [a], Hiroyuki Kisanuki [a], Ruri Kaneda [a], Jun Ota [a, f], Koji Koinuma [a], Madoka Ishikawa [a], Shuji Takada [a], Yoshihiro Yamashita [a], Kazuo Oshimi [b], Hiroyuki Mano [a, f, *]

[a] *Division of Functional Genomics, Jichi Medical School, 3311-1 Yakushiji, Kawachigun, Tochigi 329-0498, Japan*
[b] *Division of Hematology, Department of Medicine, Juntendo University School of Medicine, Tokyo, Japan*
[c] *Department of Molecular Microbiology and Immunology, Nagasaki University Graduate School of Medicine, Nagasaki, Japan*
[d] *Center for Experimental Medicine, Institute of Medical Science, University of Tokyo, Tokyo, Japan*
[e] *Second Department of Internal Medicine, Shinshu University School of Medicine, Nagano, Japan*
[f] *CREST, Japan Science and Technology Agency, Saitama, Japan*

Received 17 October 2004; accepted 22 January 2005
Available online 24 February 2005

Abstract

Aggressive natural killer cell leukemia (ANKL) is an intractable malignancy that is characterized by the outgrowth of NK cells. To identify transforming genes in ANKL, we constructed a retroviral cDNA expression library from an ANKL cell line KHYG-1. Infection of 3T3 cells with recombinant retroviruses yielded 33 transformed foci. Nucleotide sequencing of the DNA inserts recovered from these foci revealed that 31 of them encoded KRAS2 with a glycine-to-alanine mutation at codon 12. Mutation-specific PCR analysis indicated that the *KRAS* mutation was present only in KHYG-1 cells, not in another ANKL cell line or in clinical specimens ($n=8$).
© 2005 Elsevier Ltd. All rights reserved.

Keywords: Aggressive NK cell leukemia; cDNA expression library; Retrovirus; KRAS2 oncogene

1. Introduction

Outgrowth of $CD3^{-}CD16/CD56^{+}$ natural killer (NK) cells in peripheral blood is diagnosed as either chronic NK lymphocytosis (CNKL) or aggressive NK cell leukemia (ANKL) [1,2]. Whereas the former condition has an indolent clinical course with few symptoms, the latter is characterized by chemoresistance and multiorgan failure and has a poor outcome.

The Epstein–Barr virus (EBV) genome is frequently present episomally in ANKL cells [3], suggesting a role for EBV in disease pathogenesis. However, little is known of how infection with EBV might trigger clonal growth of NK cells. Inactivation of tumor suppressor genes has been associated with NK cell neoplasia. For instance, a homozygous deletion of the genes for p16INK4A, p15INK4B, or p14ARF has been detected [4]. Additionally, inactivating mutations of the FAS gene have been found in nasal NK/T cell lymphoma [5].

A few studies have identified a potential contribution of oncogenes to NK cell malignancy. Mutations that affect codons 13 or 22 of *KRAS2* were found in NK/T cell lymphoma [6] but not in ANKL [7]. Furthermore, although mutations in *KIT* were associated with NK/T cell lymphoma, transforming activity of the mutant KIT proteins was not demonstrated [8]. A role for oncogenes in ANKL has not been identified to date.

Functional screening based on transforming ability is one potential approach to the efficient isolation of tumor-promoting genes in ANKL. Focus formation assays with

* Corresponding author. Tel.: +81 285 58 7449; fax: +81 285 44 7322.
E-mail address: hmano@jichi.ac.jp (H. Mano).

0145-2126/$ – see front matter © 2005 Elsevier Ltd. All rights reserved.
doi:10.1016/j.leukres.2005.02.002

mouse 3T3 fibroblasts have indeed proved successful for the identification of oncogenes in human cancer [9]. In such screening assays, genomic DNA isolated from cancer specimens is used to transfect 3T3 cells and the formation of transformed cell foci is then evaluated. Expression of the exogenous genes in such experiments is driven by their own promoters or enhancers, however, so that oncogenes can exert transforming effects in 3T3 cells only if their regulatory regions are active in fibroblasts. Given the distinct developmental origins of NK cells and fibroblasts, expression of oncogenes associated with ANKL in 3T3 cells under these conditions is not guaranteed.

This problem might be expected to be overcome by the expression of test cDNAs under the control of an ectopic promoter in 3T3 cells. We have therefore constructed a retroviral cDNA expression library from the ANKL cell line KHYG-1 [10] and used this library to infect 3T3 cells. In preparation of the cDNA library, we took advantage of a polymerase chain reaction (PCR)-based system that preferentially amplifies full-length cDNAs. The resulting library was found to have sufficient complexity and to contain a high percentage of full-length cDNAs. Focus formation assays with 3T3 cells resulted in the identification of *KRAS2* as a transforming gene in KHYG-1 cells.

2. Materials and methods

2.1. Cell culture and clinical samples

KHYG-1 and NKL cells [11] were kindly provided by M. Yagita and Y. Yokota, respectively, and were cultured in RPMI 1640 medium (Invitrogen, Carlsbad, CA) supplemented with 10% fetal bovine serum (Invitrogen) and human interleukin-2 (20 U/mL) (Roche, St. Louis, MO). The BOSC23 packaging cell line for ecotropic retroviruses [12] and mouse 3T3 fibroblasts were maintained in Dulbecco's modified Eagle's medium (DMEM)–F12 (Invitrogen) supplemented with 10% fetal bovine serum and 2 mM L-glutamine.

Mononulear cells were isolated by Ficoll–Hypaque density gradient centrifugation from peripheral blood of the subjects with informed consent. The cells were incubated with anti-CD3 MicroBeads (Miltenyi Biotec, Auburn, CA), and loaded onto MIDI-MACS magnetic cell separation columns (Miltenyi Biotec) to remove $CD3^+$ cells. The flow-through was then mixed with anti-CD56 MicroBeads (Miltenyi Biotec), and was subjected to a MINI-MACS column for the "positive selection" of $CD56^+$ cells. Cells bound specifically to the column was then eluted according to the manufacturer's instructions.

2.2. Construction of a retrovirus library

Total RNA was extracted from KHYG-1 cells with the use of an RNeasy Mini column and RNase-free DNase (Qiagen, Valencia, CA), and first-strand cDNA was synthesized from the RNA with PowerScript reverse transcriptase, a SMART IIA oligonucleotide, and CDS primer IIA (Clontech, Palo Alto, CA). The resulting cDNA molecules were then amplified for 12 cycles with 5′-PCR primer IIA and a SMART PCR cDNA synthesis kit (Clontech), with the exception that LA Taq polymerase (Takara Bio, Shiga, Japan) was substituted for the Advantage 2 DNA polymerase provided with the kit. The PCR products were treated with proteinase K, rendered blunt-ended with T4 DNA polymerase, and ligated to a *Bst*XI adapter (Invitrogen). Unbound adapters were removed with a cDNA size fractionation column (Invitrogen), and the modified cDNAs were ligated into the pMX retroviral plasmid (kindly provided by T. Kitamura) [13] that had been digested with *Bst*XI. The pMX-cDNA plasmids were introduced into ElecroMax DH10B cells (Invitrogen) by electroporation.

2.3. Focus formation assay

BOSC23 cells (1.8×10^6) were seeded onto 6-cm culture plates, cultured for 1 day, and then transfected with a mixture comprising 2 μg of retroviral plasmids, 0.5 μg of pGP plasmid (Takara Bio), 0.5 μg of pE-eco plasmid (Takara Bio), and 18 μL of Lipofectamine reagent (Invitrogen). Two days after transfection, polybrene (Sigma, St. Louis, MO) was added at a concentration of 4 μg/mL to the culture supernatant, which was then used to infect 3T3 cells for 48 h. For the focus formation assay, the culture medium of 3T3 cells was changed to DMEM–high glucose (Invitrogen) supplemented with 5% calf serum and 2 mM L-glutamine. Transformed foci were isolated after 3 weeks of culture.

2.4. Recovery of cDNAs from 3T3 cells

Each 3T3 cell clone was harvested with a cloning syringe and cultured independently in a 10-cm culture plate. Genomic DNA was subsequently extracted from the cells and subjected to PCR with 5′-PCR primer IIA and LA Taq polymerase for 50 cycles of 98 °C for 20 s and 68 °C for 6 min. Amplified genomic fragments were purified by gel electrophoresis and ligated into the pT7Blue-2 vector (EMD Biosciences, San Diego, CA) for nucleotide sequencing.

2.5. Mutation-specific PCR for KRAS2

Detection of $KRAS2^{G12A}$ cDNA was performed as described previously [14] but with minor modifications. In brief, a 5′-region of *KRAS2* cDNA was amplified from oligo(dT)–primed cDNA by PCR with 5′-RAS primer (5′-ACTGAATATAAACTTGTGGTAGTTGGACCT-3′; the underlined cytosine was incorporated to generate a *Bst*NI site) and 3′-RAS primer A (5′-CTGTGTCGAGAATATCCAAGAGACA-3′). The PCR product was subjected to digestion with *Bst*NI (New England Biolabs, Beverly, MA) and then to a second PCR with 5′-RAS primer and 3′-RAS primer B (5′-CTGTGTCGAGAATCCAGGAGACA-3′; the under-

lined guanine was incorporated to generate a *Bst*NI site). The second PCR product was then also subjected to digestion with *Bst*NI, and the resulting DNA fragments were separated by agarose gel electrophoresis.

3. Results

3.1. Construction of a full-length cDNA expression library for KHYG-1 cells

Full-length cDNAs were selectively amplified from mRNA of KHYG-1 cells and ligated into the retroviral vector pMX. We obtained a total of 5.61×10^6 colony-forming units (cfu) of independent plasmid clones. To evaluate the quality of the library, we randomly selected 40 clones and examined the incorporated cDNAs. Thirty-nine of the 40 clones contained inserts with an average size of 2.03 kbp. The cDNA inserts from 20 out of these 39 clones were sequenced from both ends, and the determined sequences were used to screen, with the BLAT search program [15], the nucleotide sequence database assembled as of July 2003 by the Genome Bioinformatics Group of the University of California at Santa Cruz (http://genome.ucsc.edu/). Both ends of 14 of the 20 cDNAs could be matched to the mRNA sequences of known genes, and 13 of these cDNAs included complete open reading frames (data not shown). We therefore concluded that the retroviral cDNA expression library was of sufficient complexity and sufficiently enriched in full-length cDNAs for the present study.

3.2. Identification of $KRAS2^{G12A}$ in KHYG-1 cells

We generated a recombinant ecotropic retrovirus library by introducing 7.1×10^5 cfu of the generated plasmids into a packaging cell line. This library was then used to infect mouse 3T3 fibroblasts. After culture of the infected cells for 3 weeks, we detected 33 transformed foci (Fig. 1). Each focus was isolated, expanded independently, and subjected to extraction of genomic DNA for the recovery of retroviral inserts by PCR with the primer used originally to amplify the cDNAs during construction of the library. In most instances, a single major DNA fragment was recovered from each genome (Fig. 2A), suggestive of original infection of a single 3T3 cell with a single retrovirus.

The recovered cDNA fragments were sequenced from both ends for all 33 clones. Screening of the human genome sequence database with the insert sequences revealed that those from 31 of the 33 clones (#1–#29, #31, #33) matched, with >98% identity, the sequence of human *KRAS2* (GenBank accession number, NM_004985). The genome of 3T3 clone ID #30 yielded two PCR fragments (Fig. 2A); the larger (~1.4 kbp) and the smaller (~0.9 kbp) fragments were revealed to be derived from β-actin (*ACTB*; GenBank accession number, NM_001101) and profilin 1 (*PFN1*; GenBank accession number, NM_005022) genes, respectively. The final 3T3 clone (#32) yielded a major PCR fragment corresponding to the gene for isocitrate dehydrogenase 3 (NAD^+) β (*IDH3B*; GenBank accession number, NM_006899).

KRAS2 belongs to the *RAS* gene family and is involved in a wide variety of human cancers [16]. Given that point

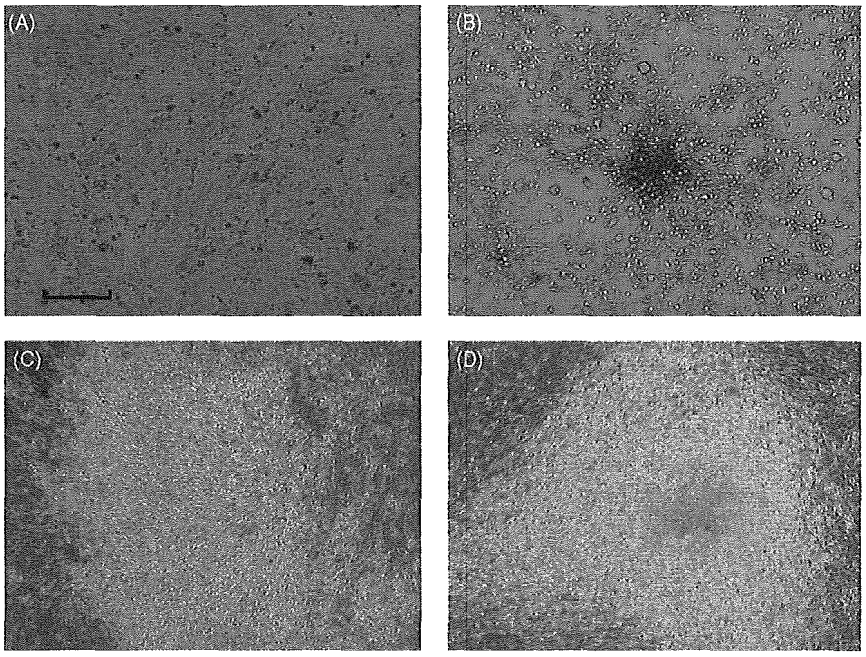

Fig. 1. Focus formation assay with a retroviral library derived from KHYG-1 cells. Mouse 3T3 cells were infected with the empty virus (A), a retrovirus expressing v-Ras as a positive control (B), or retroviruses from the KHYG-1 cell library (C and D). The cultures were photographed 3 weeks after infection. Scale bar, 100 μm.

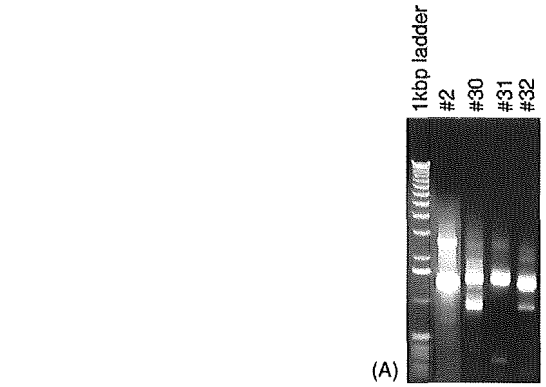

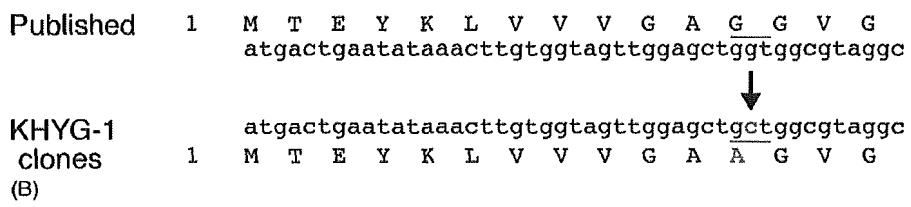

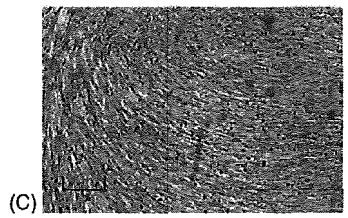

Fig. 2. Identification of a *KRAS* mutant gene with transforming activity: (A) Genomic DNA isolated from transformed 3T3 cell foci (clones #2, #30, #31, and #32) was subjected to PCR for amplification of the DNA inserts. The left lane contains DNA size markers (1-kbp DNA ladder; Invitrogen); (B) The nucleotide sequences of the DNA inserts derived from 31 of the 33 transformed foci matched that of *KRAS* with a single nucleotide substitution (G to C) in the second position of codon 12 that results in a change in the encoded amino acid from glycine to alanine; (C) A recombinant retrovirus encoding KRAS2^{G12A} was used to infect 3T3 cells. The cells were photographed after culture for 2 weeks. Scale bar, 50 μm.

mutations in *KRAS2* confer oncogenic activity, we compared the nucleotide sequences of the *KRAS2* cDNAs derived from KHYG-1 cells with the published sequence of the wild-type gene. Although oncogenic mutations have previously been shown to affect codons 12, 13, and 59 of *KRAS2*, all of the KHYG-1 cell cDNAs harbored the same mutation: the GGT sequence of codon 12 was changed to GCT, resulting in the substitution of an alanine residue for the glycine normally present at this position (Fig. 2B). To verify the transforming ability of *KRAS2*^{G12A}, we inserted the corresponding cDNA into the pMX retroviral vector and generated recombinant retroviruses for infection of 3T3 cells. The recipient 3T3 cells indeed underwent transformation (Fig. 2C), confirming that *KRAS2*^{G12A} possesses oncogenic activity.

3.3. Screening for *KRAS2*^{G12A} in NK cell leukemia

To determine whether *KRAS2*^{G12A} is frequently associated with NK cell leukemia, we applied a slightly modified version of a rapid screening method previously described by Kahn et al. [14]. *KRAS2* cDNA was first amplified by PCR with 5′-RAS primer and 3′-RAS primer A (Fig. 3A). The 3′ end of 5′-RAS primer corresponds to codon 11 of *KRAS2* but contains a cytosine substitution in the first position of codon 11, which generates a *Bst*NI recognition site [CC(T/A)GG] that includes the first and second positions of codon 12. The presence of a point mutation at the first or second position of codon 12 would therefore prevent digestion of the PCR product by *Bst*NI.

After *Bst*NI digestion, the PCR product was subjected to a second PCR with 5′-RAS primer and 3′-RAS primer B. Given that *Bst*NI digestion removes the binding site for 5′-RAS primer, only *KRAS2* cDNA with a mutation at the first or second position of codon 12 should yield a second PCR product. Even if *Bst*NI digestion of the initial PCR product was not complete and the second PCR amplified a trace amount of wild-type *KRAS2* cDNA, a second *Bst*NI digestion further discriminates between the wild-type and mutant genes. The 3′-RAS primer B thus contains a guanine substitution that generates a *Bst*NI site. The second PCR product of wild-type *KRAS2* cDNA would thus contain two *Bst*NI sites, whereas that of mutant *KRAS2* contains only one.

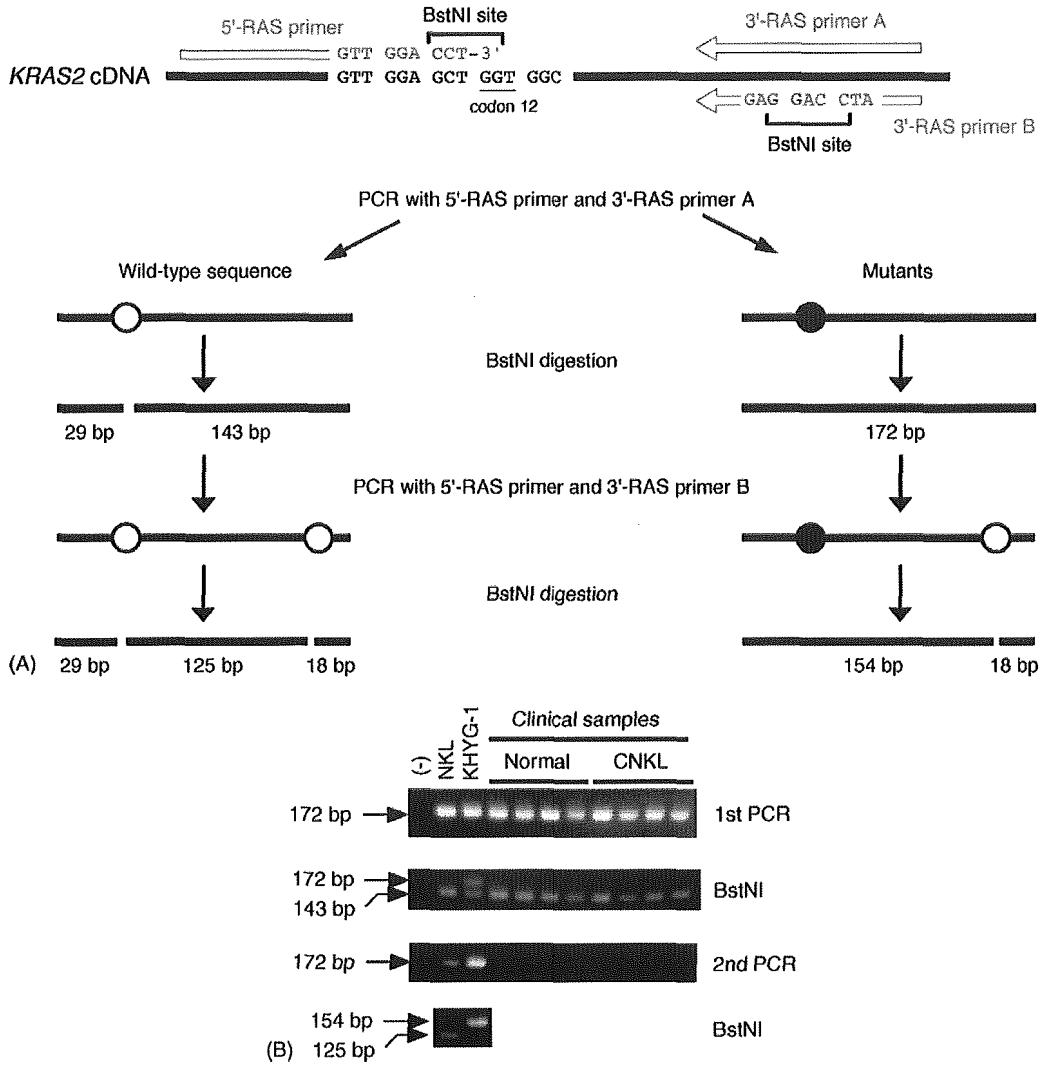

Fig. 3. Mutation-specific PCR analysis of NK cell leukemia cell lines and clinical specimens: (A) *KRAS2* cDNA was amplified with 5′-RAS primer and 3′-RAS primer A. The PCR product was subjected to digestion with *Bst*NI and then to a second PCR with 5′-RAS primer and 3′-RAS primer B. The second PCR product was also subjected to digestion with *Bst*NI. The nucleotides shown in red were incorporated into the primers to generate a *Bst*NI site. Open circles indicate *Bst*NI sites; closed circles indicate corresponding mutant sequences that are not susceptible to *Bst*NI; (B) cDNA isolated from the NKL and KHYG-1 cell lines as well as from $CD3^{-}CD56^{+}$ NK cell fractions derived from healthy volunteers (Normal) or individuals with CNKL was subjected to mutation-specific PCR analysis. A reaction without input DNA was also performed as a negative control (–). The size of DNA fragments is indicated on the left.

With this approach, we analyzed cDNA prepared from two ANKL cell lines (NKL and KHYG-1) and from $CD3^{-}CD56^{+}$ NK cell fractions purified from the peripheral blood of healthy individuals ($n=4$) and patients with CNKL ($n=4$). The first PCR step yielded a single DNA fragment of 172 bp from all samples. Furthermore, only the PCR product from KHYG-1 cells was refractory to *Bst*NI digestion, indicating that only KHYG-1 cells harbor a codon 12 mutation of *KRAS2*. The presence of the 143-bp band may indicate that KHYG-1 cells are heterozygous for the *KRAS2* mutation. The second PCR generated a 172-bp DNA fragment only with the NKL and KHYG-1 cell samples. Whereas this fragment derived from NKL cells was completely digested by *Bst*NI to generate a 125-bp band, *Bst*NI digestion of the fragment derived from KHYG-1 cells generated a band of 154 bp. Of all the samples analyzed, therefore, mutation of the first or second position of codon 12 of *KRAS2* was detected only in KHYG-1 cells.

4. Discussion

We have constructed a retroviral cDNA expression library for an ANKL cell line. Given that >97% (39/40) of the viral plasmids contained cDNA inserts and that the overall clone number was $>5 \times 10^6$, our library likely represents most of

the transcriptome of KHYG-1 cells. The high probability that the incorporated cDNAs are full length is also an important advantage for functional screening.

In our screening, most of the 3T3 transformants were found to have incorporated a single cDNA fragment corresponding to *KRAS2*^{G12A}, with only two transformants found to contain other cDNAs. One of these two cDNA inserts was derived from the gene for PFN1, a protein that binds to unpolymerized actin [17]. Homozygous deletion of *Pfn1* results in embryonic death in mice, with the encoded protein apparently being indispensable for cell growth or differentiation during embryonic development [18]. The other cDNA insert isolated from 3T3 transformants contained the entire open reading frame for IDH3B, which catalyzes the oxidative decarboxylation of isocitrate and is a key enzyme in the tricarboxylic acid cycle [19]. Neither *PFN1* nor *IDH3B* has previously been shown to possess oncogenic activity. It is currently under examination whether a long terminal repeat (LTR)-driven overexpression of *PFN1* or *IDH3B* leads focus formation in 3T3 cells.

Comparative genomic hybridization analysis identified a wide variety of genetic alterations at a high frequency in ANKL cells [20], suggesting that leukemogenesis in ANKL is associated with multiple steps of oncogene activation. An analysis of patients with NK cell neoplasia failed to detect any changes in the genes for members of the RAS and MYC families of proteins [7], however. This previous study did find a frequent increase in the abundance of the cell cycle regulator MDM2.

In contrast, we have detected a transforming *KRAS2* mutant gene in an ANKL cell line. Given that the mutation in codon 12 of this gene was detected by two different approaches (retroviral screening of PCR-amplified cDNAs and mutation-specific PCR), we conclude that it was not an artifact of PCR. KRAS2 is a GTP-binding protein with a relative molecular mass of ~21 kDa. Together with HRAS and NRAS, it plays an important role in cell growth and differentiation. Many mitogenic signals promote the loading of KRAS2 with GTP, which in turn triggers various downstream signaling events including activation of the mitogen-activated protein kinase (MAPK) pathway.

Activating mutations of *KRAS2* have been identified in a wide range of human cancers. Mutations of codon 12, for example, are associated with acute lymphoblastic leukemia [21], lung cancer [22], and pancreatic cancer [23]. No such mutations have previously been detected in association with ANKL, however. Although we have now identified a *KRAS2* mutation affecting codon 12 in the ANKL cell line KHYG-1, we did not detect this mutation in another ANKL cell line (NKL) or in $CD3^{-}CD56^{+}$ NK cell fractions isolated from healthy volunteers or from individuals with CNKL. Mutation of *KRAS2*, at least of codon 12 of this gene, might therefore be an infrequent event in NK cell neoplasia. Indeed, it remains possible that the detected *KRAS2* mutation is specific to the KHYG-1 cell line. Nevertheless, our identification of an activating *KRAS2* mutation in KHYG-1 cells might provide insight into the role of the RAS-MAPK signaling pathway in ANKL carcinogenesis. Furthermore, given the high quality of our retroviral expression library, the strategy adopted in the present study also might prove useful for the functional screening of genes associated with various clinical characteristics of ANKL, such as chemoresistance.

Acknowledgments

This work was supported in part by grants for Research on Human Genome and Tissue Engineering and for Third-Term Comprehensive Control Research for Cancer from the Ministry of Health, Labor, and Welfare of Japan, as well as by grants from Research Foundation for Community Medicine of Japan, Sankyo Foundation of Life Science, Takeda Science Foundation, and Mitsubishi Pharma Research Foundation. Y.-L.C conducted most of the experiments. R.M., M.O., A.I. and T.W. helped to establish a retroviral expression library. Hideki Makishima, J.O. and K.O. collected the ANKL specimens, and conducted the mutation-specific PCR method. H.K., R.K., K.K., M.I., S.T. and Y.Y. helped the 3T3 focus formation screening, and provided suggestions on molecular biology. Hiroyuki Mano designed this project with Y.-L.C., and was responsible for all aspects of this project.

References

[1] Harris NL, Jaffe ES, Diebold J, Flandrin G, Muller-Hermelink HK, Vardiman J, et al. World Health Organization classification of neoplastic diseases of the hematopoietic and lymphoid tissues: report of the Clinical Advisory Committee meeting, Airlie House, Virginia, November. J Clin Oncol 1999;17:3835–49.

[2] Oshimi K. Leukemia and lymphoma of natural killer lineage cells. Int J Hematol 2003;78:18–23.

[3] Gelb AB, van de Rijn M, Regula Jr DP, Cornbleet JP, Kamel OW, Horoupian DS, et al. Epstein–Barr virus-associated natural killer-large granular lymphocyte leukemia. Hum Pathol 1994;25:953–60.

[4] Sakajiri S, Kawamata N, Egashira M, Mori K, Oshimi K. Molecular analysis of tumor suppressor genes, Rb, p53, p16INK4A, p15INK4B and p14ARF in natural killer cell neoplasms. Jpn J Cancer Res 2001;92:1048–56.

[5] Takakuwa T, Dong Z, Nakatsuka S, Kojya S, Harabuchi Y, Yang WI, et al. Frequent mutations of Fas gene in nasal NK/T cell lymphoma. Oncogene 2002;21:4702–5.

[6] Hoshida Y, Hongyo T, Nakatsuka S, Nishiu M, Takakuwa T, Tomita Y, et al. Gene mutations in lymphoproliferative disorders of T and NK/T cell phenotypes developing in renal transplant patients. Lab Invest 2002;82:257–64.

[7] Sugimoto KJ, Kawamata N, Sakajiri S, Oshimi K. Molecular analysis of oncogenes, ras family genes (N-ras, K-ras, H-ras), myc family genes (c-myc, N-myc) and mdm2 in natural killer cell neoplasms. Jpn J Cancer Res 2002;93:1270–7.

[8] Hongyo T, Li T, Syaifudin M, Baskar R, Ikeda H, Kanakura Y, et al. Specific c-kit mutations in sinonasal natural killer/T-cell lymphoma in China and Japan. Cancer Res 2000;60:2345–7.

[9] Aaronson SA. Growth factors and cancer. Science 1991;254:1146–53.

[10] Yagita M, Huang CL, Umehara H, Matsuo Y, Tabata R, Miyake M, et al. A novel natural killer cell line (KHYG-1) from a patient with aggressive natural killer cell leukemia carrying a p53 point mutation. Leukemia 2000;14:922–30.
[11] Robertson MJ, Cochran KJ, Cameron C, Le JM, Tantravahi R, Ritz J, et al. Characterization of a cell line, NKL, derived from an aggressive human natural killer cell leukemia. Exp Hematol 1996;24:406–15.
[12] Pear WS, Nolan GP, Scott ML, Baltimore D. Production of high-titer helper-free retroviruses by transient transfection. Proc Natl Acad Sci USA 1993;90:8392–6.
[13] Onishi M, Kinoshita S, Morikawa Y, Shibuya A, Phillips J, Lanier LL, et al. Applications of retrovirus-mediated expression cloning. Exp Hematol 1996;24:324–9.
[14] Kahn SM, Jiang W, Culbertson TA, Weinstein IB, Williams GM, Tomita N, et al. Rapid and sensitive nonradioactive detection of mutant K-ras genes via 'enriched' PCR amplification. Oncogene 1991;6:1079–83.
[15] Kent WJ. BLAT—the BLAST-like alignment tool. Genome Res 2002;12:656–64.
[16] Ayllon V, Rebollo A. Ras-induced cellular events. Mol Membr Biol 2000;17:65–73.
[17] Goldschmidt-Clermont PJ, Janmey PA, Profilin. A weak CAP for actin and RAS. Cell 1991;66:419–21.
[18] Witke W, Sutherland JD, Sharpe A, Arai M, Kwiatkowski DJ. Profilin I is essential for cell survival and cell division in early mouse development. Proc Natl Acad Sci USA 2001;98:3832–6.
[19] Kim YO, Park SH, Kang YJ, Koh HJ, Kim SH, Park SY, et al. Assignment of mitochondrial NAD(+)-specific isocitrate dehydrogenase beta subunit gene (IDH3B) to human chromosome band 20p13 by in situ hybridization and radiation hybrid mapping. Cytogenet Cell Genet 1999;86:240–1.
[20] Siu LL, Wong KF, Chan JK, Kwong YL. Comparative genomic hybridization analysis of natural killer cell lymphoma/leukaemia. Recognition of consistent patterns of genetic alterations. Am J Pathol 1999;155:1419–25.
[21] Perentesis JP, Bhatia S, Boyle E, Shao Y, Shu XO, Steinbuch M, et al. RAS oncogene mutations and outcome of therapy for childhood acute lymphoblastic leukemia. Leukemia 2004;18:685–92.
[22] Santos E, Martin-Zanca D, Reddy EP, Pierotti MA, Della Porta G, Barbacid M. Malignant activation of a K-ras oncogene in lung carcinoma but not in normal tissue of the same patient. Science 1984;223:661–4.
[23] Motojima K, Urano T, Nagata Y, Shiku H, Tsurifune T, Kanematsu T. Detection of point mutations in the Kirsten-ras oncogene provides evidence for the multicentricity of pancreatic carcinoma. Ann Surg 1993;217:138–43.

Available online at www.sciencedirect.com
SCIENCE DIRECT®
Biochemical and Biophysical Research Communications 338 (2005) 1256–1262
BBRC
www.elsevier.com/locate/ybbrc

Transforming activity of the lymphotoxin-β receptor revealed by expression screening

Shin-ichiro Fujiwara [a,b,c], Yoshihiro Yamashita [a], Young Lim Choi [a], Tomoaki Wada [a], Ruri Kaneda [a,d], Shuji Takada [a], Yukio Maruyama [c], Keiya Ozawa [b], Hiroyuki Mano [a,d,*]

[a] *Division of Functional Genomics, Jichi Medical School, Tochigi 329-0498, Japan*
[b] *Division of Hematology, Jichi Medical School, Tochigi 329-0498, Japan*
[c] *First Department of Internal Medicine, Fukushima Medical University, Fukushima 960-1295, Japan*
[d] *CREST, Japan Science and Technology Agency, Saitama 332-0012, Japan*

Received 13 October 2005
Available online 24 October 2005

Abstract

Pancreatic ductal carcinoma (PDC) remains one of the most intractable human malignancies. To obtain insight into the molecular pathogenesis of PDC, we constructed a retroviral cDNA expression library with total RNA isolated from the PDC cell line MiaPaCa-2. Screening of this library with the use of a focus formation assay with NIH 3T3 mouse fibroblasts resulted in the identification of 13 independent genes with transforming activity. One of the cDNAs thus identified encodes an NH_2-terminally truncated form of the lymphotoxin-β receptor (LTBR). The transforming activity of this short-type LTBR in 3T3 cells was confirmed by both an in vitro assay of cell growth in soft agar and an in vivo assay of tumorigenicity in nude mice. The full-length (wild-type) LTBR protein was also found to manifest similar transforming activity. These observations suggest that LTBR, which belongs to the tumor necrosis factor receptor superfamily of proteins, may contribute to human carcinogenesis.
© 2005 Elsevier Inc. All rights reserved.

Keywords: Lymphotoxin-β receptor; Pancreatic ductal carcinoma; Retrovirus; cDNA expression library; Oncogene

Pancreatic ductal carcinoma (PDC) originates from pancreatic ductal cells and remains one of the most intractable human malignancies [1,2]. Effective therapy for PDC is hampered by the absence of specific clinical symptoms. At the time of diagnosis, most affected individuals are no longer candidates for surgical resection, and, even in patients who do undergo such surgery, the 5-year survival rate is only 20–30% [2].

The molecular pathogenesis of PDC has been the subject of intensive investigation. The gene *KRAS2* is frequently mutated and activated in PDC cells [3], and various tumor suppressor genes, including those for p53, p16, and BRCA2, are inactivated [4]. Furthermore, genetic or epigenetic alterations of genes important in apoptosis or in tumor cell invasion or metastasis have been detected in PDC cells [5]. However, mutations in *KRAS2* have also been identified in pancreatic tissue affected by nonmalignant chronic pancreatitis [6], and genetic changes truly specific to PDC remain to be uncovered. Improvement in the prognosis of individuals with PDC will require identification of the genetic or epigenetic alterations responsible for the aggressive nature of this cancer.

The focus formation assay with 3T3 or RAT1 fibroblasts has been extensively used to screen for transforming genes in various carcinomas [7]. Given that the expression of exogenous genes in this assay is usually controlled by their own promoters or enhancers, however, oncogenes are able to exert their transforming effects in the recipient cells only if these regulatory regions are active in fibroblasts, which is not always the case. Regulation of the transcription of test cDNAs by a promoter known to function efficiently in fibroblasts would be expected to

* Corresponding author. Fax: +81 285 44 7322.
E-mail address: hmano@jichi.ac.jp (H. Mano).

0006-291X/$ - see front matter © 2005 Elsevier Inc. All rights reserved.
doi:10.1016/j.bbrc.2005.10.080

ensure sufficient expression of the encoded protein in the focus formation assay. We have therefore now constructed a retroviral cDNA expression library from a human PDC cell line, MiaPaCa-2, and tested this library in the focus formation assay with 3T3 cells. For library construction, we took advantage of a polymerase chain reaction (PCR) system that preferentially amplifies full-length cDNAs. The resulting library had sufficient complexity with a high percentage of full-length cDNAs. With this library, we have revealed that the lymphotoxin-β receptor (LTBR) gene possesses transforming activity.

Materials and methods

Cell lines and culture. MiaPaCa-2, NIH 3T3, and BOSC23 cell lines were obtained from American Type Culture Collection and maintained in Dulbecco's modified Eagle's medium (DMEM)–F12 (Invitrogen, Carlsbad, CA) supplemented with 10% fetal bovine serum (Invitrogen) and 2 mM L-glutamine.

Construction of retroviral cDNA expression library. Total RNA extracted from MiaPaCa-2 cells with the use of an RNeasy Mini column and RNase-free DNase (Qiagen, Valencia, CA) was subjected to first-strand cDNA synthesis with PowerScript reverse transcriptase, SMART IIA oligonucleotide, and CDS primer IIA (Clontech, Palo Alto, CA). The resulting cDNAs were amplified for 14 cycles with 5′ PCR primer IIA and a SMART PCR cDNA synthesis kit (Clontech), with the exception that LA *Taq* polymerase (Takara Bio, Shiga, Japan) was substituted for the Advantage 2 DNA polymerase provided with the kit. The amplified cDNAs were treated with proteinase K, rendered blunt-ended with T4 DNA polymerase, and ligated to the BstXI-adaptor (Invitrogen). Unbound adaptors were removed with the use of a cDNA size-fractionation column (Invitrogen), and the remaining cDNAs were ligated into the BstXI site of the pMXS retroviral plasmid (kindly provided by T. Kitamura, Institute of Medical Science, University of Tokyo). The resulting pMXS-cDNA plasmids were introduced into ElecroMax DH10B cells (Invitrogen) by electroporation.

Focus formation assay. BOSC23 cells (1.8×10^6) were seeded into a 6-cm culture dish, cultured for 24 h, and then transfected with 2 μg of retroviral plasmids mixed with 0.5 μg of pGP plasmid (Takara Bio), 0.5 μg of pE-eco plasmid (Takara Bio), and 18 μl of Lipofectamine reagent (Invitrogen). Two days after transfection, polybrene (Sigma, St. Louis, MO) was added to the culture supernatant at a concentration of 4 μg/ml, and the supernatant was subsequently used to infect 3T3 cells for 48 h. The culture medium of the 3T3 cells was then changed to DMEM-F12 supplemented with 5% calf serum and 2 mM L-glutamine, and the cells were cultured for 2 weeks.

Recovery of cDNAs from transformants. Transformed 3T3 cell clones were harvested with a cloning syringe and cultured independently in 10-cm culture dishes. Genomic DNA was extracted from each clone by standard procedures and then subjected to PCR with 5′ PCR primer IIA and LA *Taq* polymerase for 50 cycles of 98 °C for 20 s and 68 °C for 6 min. Amplified DNA fragments were purified by gel electrophoresis and ligated into the pT7Blue-2 vector (EMD Biosciences, San Diego, CA) for nucleotide sequencing.

Anchorage-independent growth in soft agar. 3T3 cells (2×10^6) were infected with a retrovirus encoding a truncated form of LTBR or activated KRAS2 (see Results), resuspended in the culture medium supplemented with 0.4% agar [SeaPlaque GTG agarose (Cambrex, East Rutherford, NJ)], and seeded onto a base layer of complete medium supplemented with 0.5% agar. Cell growth was assessed after culture for 2 weeks.

Tumorigenicity assay in nude mice. 3T3 cells (2×10^6) infected with a retrovirus either encoding the truncated form of LTBR or containing the human wild-type LTBR cDNA (GeneCopoeia, Germantown, MD) were resuspended in 500 μl of phosphate-buffered saline and injected into each shoulder of a nu/nu Balb-c mouse (6-weeks old). Tumor formation was assessed after 3 weeks.

5′-Rapid amplification of cDNA ends (RACE). 5′-RACE was performed as described [8]. In brief, total RNA extracted from MiaPaCa-2 cells was used to generate cDNAs with an LTBR-specific primer (5′-GCAGTGGCTGTACCAAGTCA-3′). Excess primer was removed with a microconcentrator (Amicon, Austin, TX), and a poly(A) tail was added to the cDNAs by incubation with dATP and terminal deoxynucleotidyltransferase (Invitrogen). The first PCR was performed with the dT-adaptor primer (5′-GACTCGAGTCGACATCGATTTTTTTTTTTTT TTTT-3′) and RACE-1 antisense primer (5′-CTCCCAGCTTCCAGCT ACAG-3′), and the second PCR with the adaptor primer (5′-GACTCGA GTCGACATCG-3) and RACE-2 antisense primer (5′-GAGCAGAAA GAAGGCCAGTG-3′). The amplification protocol for the first PCR comprised incubation at 94 °C for 2 min followed by 20 cycles of 94 °C for 1 min, 55 °C for 1 min, and 72 °C for 3 min. That for the second PCR included incubation at 94 °C for 2 min followed by 30 cycles of 94 °C for 1 min, 53 °C for 1 min, and 72 °C for 3 min.The final PCR products were ligated into pT7Blue-2 for nucleotide sequencing.

Results

Screening for transforming genes by focus formation assay

To screen for transforming genes in PDC, we constructed a cDNA expression library from MiaPaCa-2 cells. Full-length cDNAs were selectively amplified by a PCR protocol from total RNA isolated from the cells and were ligated into the retroviral vector pMXS. We obtained a total of 1.2×10^6 colony-forming units of independent library clones, from which we randomly selected 30 clones and examined the incorporated cDNAs. An insert of $\geqslant 500$ bp was present in 24 (80%) of the 30 clones and the average size of these 24 inserts was 1.84 kbp.

Introduction of the library plasmids into a packaging cell line yielded a recombinant retroviral library that was used to infect mouse NIH 3T3 fibroblasts. After culture of the infected cells for 2 weeks, a total of 18 transformed foci were identified. No foci were observed for 3T3 cells infected with the empty virus. Each transformed focus was isolated, expanded, and used to prepare genomic DNA. PCR amplification of the inserts identified a total of 29 cDNA fragments, each of which was ligated into a cloning vector and subjected to nucleotide sequencing from both ends. Screening of the 29 cDNA sequences against the public nucleotide sequence databases revealed that they showed >95% sequence identity to 13 independent genes, 11 known and 2 unknown (Table 1).

To confirm the transforming ability of the isolated cDNAs, we again ligated them into pMXS and used the corresponding retroviral vectors to re-infect 3T3 cells. Two of the 13 independent genes (clone ID #4, corresponding to *LTBR* [GenBank Accession No. NM_002342]; clone ID #10, corresponding to *KRAS2* [GenBank Accession No. NM_004985]) reproducibly induced the formation of transformed foci in 3T3 cells (Fig. 1). Further sequencing our *KRAS2* cDNA revealed that it has a point mutation leading to the amino acid change from a glycine residue at position 12 to a cysteine (data not shown). Whereas the oncogenic potential of mutated *KRAS2* has been

Table 1
MiaPaCa-2 cell cDNAs isolated from 3T3 transformants

Clone ID #	Gene symbol	GenBank No.	Presence of entire ORF
1	CGI-152	NM_020410	Yes
2	RAB28	NM_004249	Yes
3	MRPL43	NM_032112	Yes
4	LTBR	NM_002342	No
5	UBQLN1	NM_013438	Yes
6	TBC1D2	NM_018421	Yes
7	FKBP10	NM_021939	Yes
8	HCCA2	NM_053005	Yes
9	Unknown	AK123415	ND
10	KRAS2	NM_004985	Yes
11	STK11IP	NM_052902	Yes
12	Unknown	AA627562	ND
13	PFKP	NM_002627	Yes

ORF, open reading frame; ND, not determined.

extensively investigated [3], little is known of such activity for *LTBR*. We thus focused on *LTBR* for further analysis.

Identification of a truncated form of LTBR

Although the nucleotide sequence of both ends of our LTBR cDNA was identical to that of human *LTBR*, the size of our cDNA (1452 bp) was smaller than that (2136 bp) of the full-length cDNA previously described. We thus determined the complete nucleotide sequence of our cDNA, revealing that it starts at nucleotide position 685 of the reported sequence (NM_002342). The longest open reading frame in our cDNA begins at amino acid position 221 and ends at position 435 of the previously described LTBR protein; it therefore encodes a predicted protein of 215 amino acids with a calculated molecular mass of 22,692 Da (Fig. 2). Given that the nucleotide sequence surrounding the putative translation start site of our cDNA matches the consensus Kozak motif, the corresponding mRNA likely produces this NH_2-terminally truncated form of LTBR, which is hereafter referred to as short-type LTBR.

5′-RACE analysis of LTBR mRNA

To confirm the presence of an mRNA encoding short-type LTBR in MiaPaCa-2 cells, we performed 5′-RACE to determine the 5′ ends of LTBR mRNAs. The first strand of LTBR cDNAs was generated with an LTBR-specific reverse transcription (RT) primer (Fig. 2) from RNA isolated from MiaPaCa-2 cells. Poly(A) was added to the 3′ end of the cDNAs, which were then subjected to nested PCR in order to amplify the 5′ ends. PCR products (ranging from a few hundred to 2000 bp) were detected only when reverse transcriptase was included in the procedure (Fig. 3A), indicating that the products were synthesized from cDNA, not from genomic DNA. The nucleotide sequence of 96 randomly chosen PCR products was determined. Sixty-eight of the 96 products matched the LTBR cDNA sequence and the positions of their 5′ ends are indicated in Fig. 3B. Transcription of most of the mRNAs corresponding to these PCR products was initiated in the region immediately upstream of the translation start site for short-type LTBR, indicating the existence of multiple mRNAs for this truncated protein in vivo.

Confirmation of transforming activity of short-type LTBR

To confirm the transforming activity of short-type LTBR, we examined its effect on anchorage-independent growth of 3T3 cells in soft agar. Whereas cells infected with an empty virus did not grow in soft agar, those infected with a virus encoding short-type LTBR formed multiple foci in repeated experiments (Fig. 4A). In addition, 3T3 cells expressing activated *KRAS2* readily grew in the agar.

We also injected the infected cells into nude mice. Tumors formed at all ($n = 10$) sites injected with 3T3 cells expressing short-type LTBR (Fig. 4B). Again, 3T3 cells expressing activated *KRAS2* also generated tumors at a high frequency, whereas those infected with the empty virus did not induce tumor formation. Together, these results thus confirmed that short-type LTBR possesses transforming activity.

Transforming activity of wild-type LTBR

To determine whether the full-length (435-amino acid) LTBR protein also possesses oncogenic potential, we performed the focus formation assay and in vivo tumorigenicity assay with a recombinant retrovirus encoding the wild-type

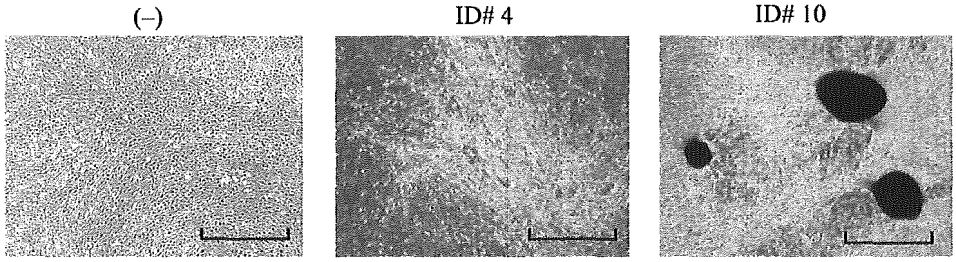

Fig. 1. Identification of transforming genes of MiaPaCa-2 cells. Mouse 3T3 cells were infected with an empty retrovirus (–) or with recombinant retroviruses harboring cDNAs corresponding to library clones ID #4 (short-type LTBR) or ID #10 (KRAS2). The cells were photographed after culture for 2 weeks. Scale bars, 1 mm.

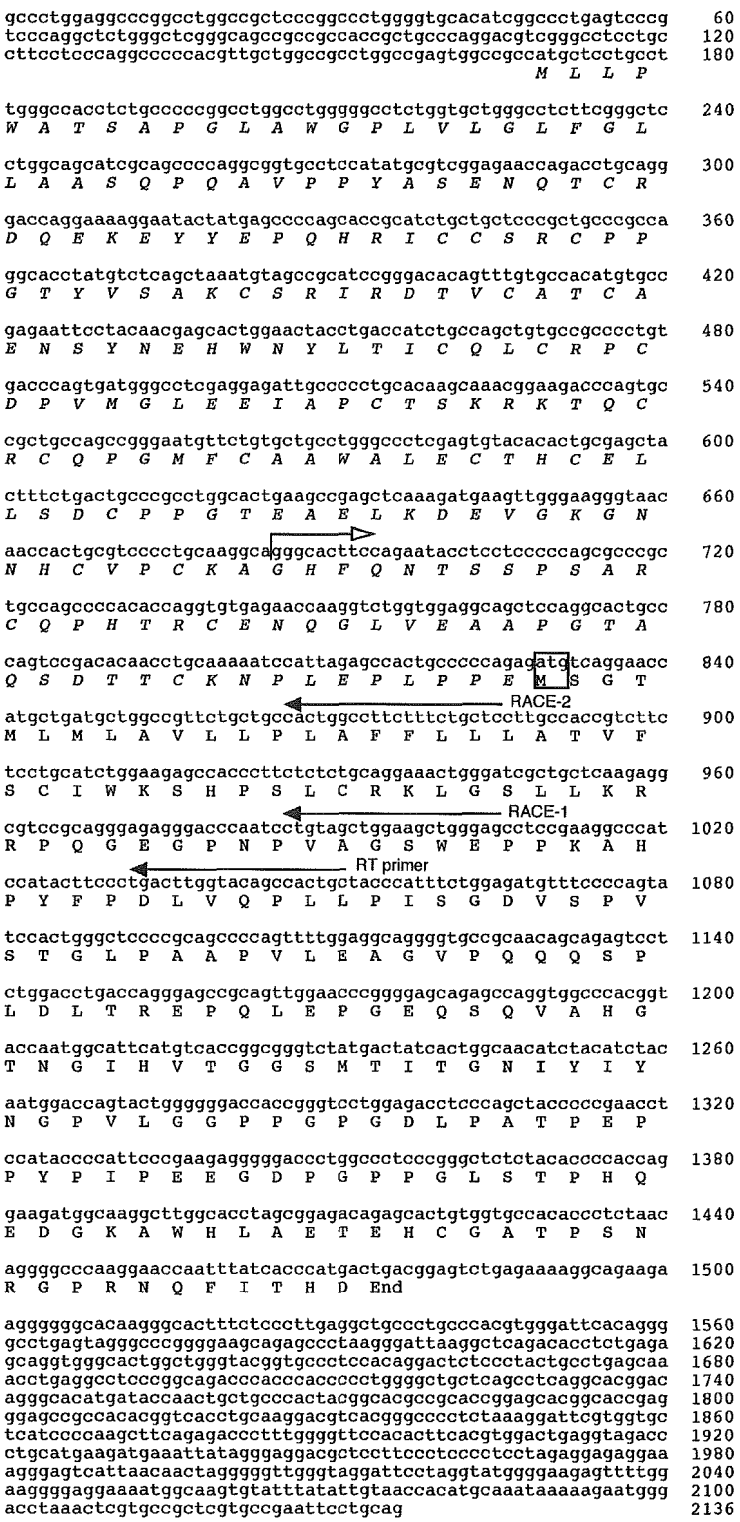

Fig. 2. Characterization of an LTBR cDNA isolated by screening for transformation activity. Amino acid residues of the full-length LTBR protein are aligned with the previously determined nucleotide sequence of LTBR cDNA (NM_002342). The cDNA isolated in the present study begins at nucleotide position 685 (open arrow) of the reported cDNA. The putative translation start site for the truncated (short-type) LTBR protein is boxed. The positions of primers used for 5′-RACE are indicated by closed arrows.

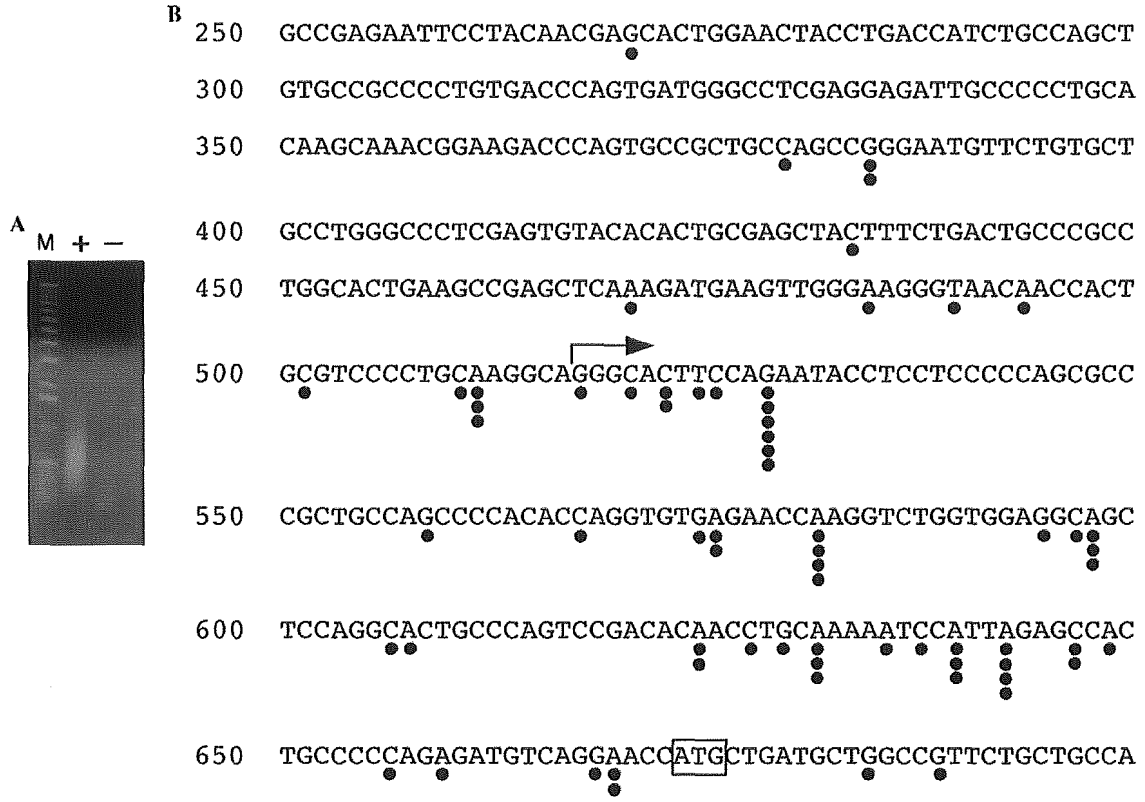

Fig. 3. 5′-RACE analysis of LTBR cDNA. (A) Total RNA of MiaPaCa-2 cells was incubated with the LTBR-specific RT primer in the presence (+) or absence (−) of reverse transcriptase, and resulting cDNA was subjected to PCR-based 5′-RACE. The PCR products were fractionated by electrophoresis through a 1.8% agarose gel and stained with ethidium bromide. Lane M, 1-kb DNA ladder. (B) The positions of the 5′ ends of 5′-RACE products are indicated by closed circles in alignment with the reported LTBR cDNA sequence. Numbers on the left indicate nucleotide positions relative to the translation initiation site of the full-length (wild-type) cDNA. The arrow indicates the 5′ end of the cDNA isolated by retroviral screening in the present study; the putative translation start codon of this cDNA is boxed.

human protein. The infected cells generated both transformed foci in vitro and tumors in nude mice (Fig. 5).

Discussion

In the present study, we constructed a retroviral cDNA expression library for a PDC cell line. Given that 80% (24/30) of the viral plasmids contained cDNA inserts and that the overall clone number was >1 million, this library should represent most of the mRNAs in MiaPaCa-2 cells. We infected 3T3 mouse fibroblasts with this recombinant library to screen for transforming genes with a focus formation assay. This screen identified *KRAS2* with an activating mutation as a transforming gene of MiaPaCa-2 cells, supporting the fidelity of our approach.

Our screen also identified a transforming cDNA that encodes an NH_2-terminally truncated form of LTBR. 5′-RACE analysis revealed the existence of mRNAs for this short-type LTBR in MiaPaCa-2 cells, and retrovirus-mediated expression of the isolated cDNA in 3T3 cells conferred the ability to grow in soft agar in vitro as well as the ability to form tumors in vivo.

LTBR belongs to the tumor necrosis factor (TNF) receptor superfamily [9] and binds two functional ligands, lymphotoxin-α1β2 and LIGHT [10,11]. LTBR is expressed by many cell types (but not by lymphocytes), whereas expression of the LTBR ligands is restricted to activated lymphocytes [11]. Signaling by LTBR is important in the development of lymphoid tissue and in generation of adaptive humoral immune responses [12,13]. In general, LTBR function is thought to be linked to apoptosis. Indeed, activation of LTBR by its endogenous ligands or by anti-receptor antibodies triggers the death of various tumor cell lines [14,15]. Activation of the LIGHT-LTBR signaling pathway in tumor cells also induces marked chemokine-dependent recruitment of T cells to tumors, resulting in the rejection of established tumor cells [16].

LTBR activation has also been linked to tumor development, however. Its activation in fibrosarcoma cells thus induces angiogenesis and tumor growth by triggering the release of macrophage inflammatory protein-2, an angiogenic CXC chemokine [17]. Although oncogenic potential has not previously been demonstrated for LTBR, our data now show that both the full-length and truncated forms of this protein possess transforming activity even in the absence of exogenous cognate ligands. A high level of expression of LTBR conferred by the retroviral long terminal repeat in our experiments might have resulted in self-oligomerization

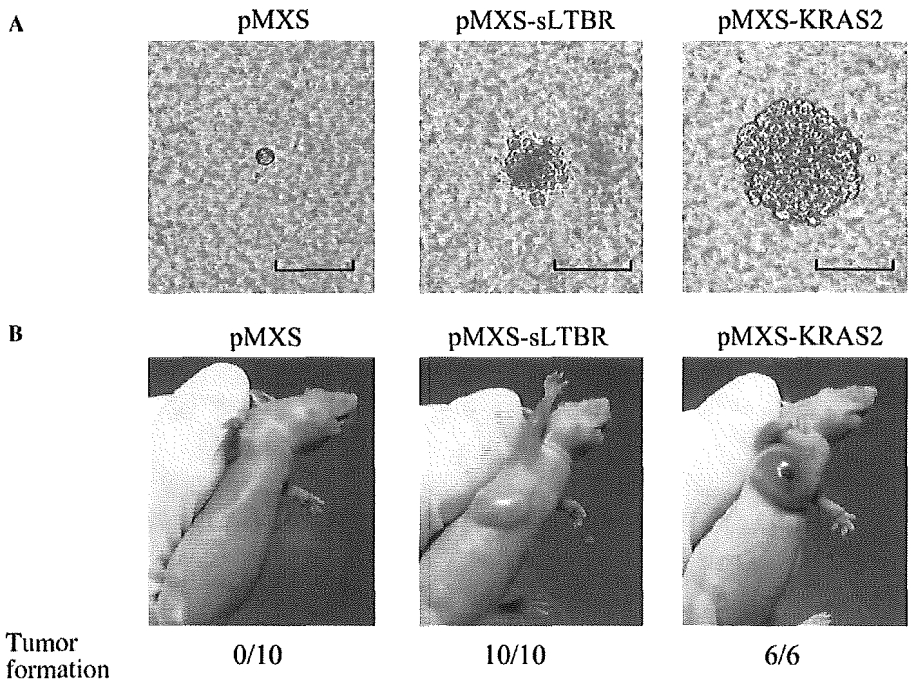

Fig. 4. Transforming activity of short-type LTBR. (A) Focus formation assay. 3T3 cells infected either with empty retrovirus (pMXS) or with retroviruses encoding short-type LTBR (pMXS-sLTBR) or activated KRAS2 (pMXS-KRAS2) were seeded into soft agar and incubated for 2 weeks. Scale bars, 100 μm. (B) Tumorigenicity assay. Cells infected as in (A) were injected into the shoulder of nude mice and tumor formation was examined after 3 weeks. The frequency of tumor formation determined is indicated.

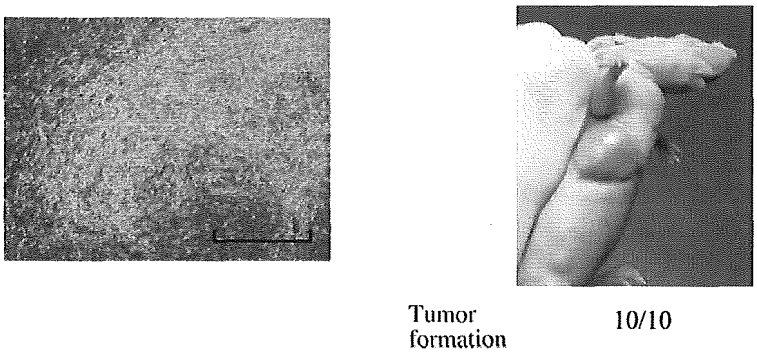

Fig. 5. Transforming activity of full-length LTBR. The transforming activity of a retroviral vector encoding full-length (wild-type) LTBR was evaluated by the focus formation assay (left) or the in vivo tumorigenicity assay (right). Scale bar, 1 mm.

of the protein. It is thus likely that LTBR exerts its oncogenic function in a tissue- and context-dependent manner. As shown here for PDC, it will be important to determine whether LTBR also contributes to the mechanism of transformation in other human malignancies.

Acknowledgments

This work was supported in part by a grant for Third-Term Comprehensive Control Research for Cancer from the Ministry of Health, Labor, and Welfare of Japan as well as by a grant for "High-Tech Research Center" Project for Private Universities: Matching Fund Subsidy (2002–2006) from the Ministry of Education, Culture, Sports, Science and Technology of Japan.

References

[1] S. Rosewicz, B. Wiedenmann, Pancreatic carcinoma, Lancet 349 (1997) 485–489.
[2] P.C. Bornman, I.J. Beckingham, Pancreatic tumours, Br. Med. J. 322 (2001) 721–723.
[3] M. Tada, M. Omata, M. Ohto, Clinical application of ras gene mutation for diagnosis of pancreatic adenocarcinoma, Gastroenterology 100 (1991) 233–238.
[4] S.R. Bramhall, The use of molecular technology in the differentiation of pancreatic cancer and chronic pancreatitis, Int. J. Pancreatol. 23 (1998) 83–100.

[5] G. Schneider, J.T. Siveke, F. Eckel, R.M. Schmid, Pancreatic cancer: basic and clinical aspects, Gastroenterology 128 (2005) 1606–1625.
[6] A. Yanagisawa, K. Ohtake, K. Ohashi, M. Hori, T. Kitagawa, H. Sugano, Y. Kato, Frequent c-Ki-ras oncogene activation in mucous cell hyperplasias of pancreas suffering from chronic inflammation, Cancer Res. 53 (1993) 953–956.
[7] S.A. Aaronson, Growth factors and cancer, Science 254 (1991) 1146–1153.
[8] M.A. Frohman, M.K. Dush, G.R. Martin, Rapid production of full-length cDNAs from rare transcripts: amplification using a single gene-specific oligonucleotide primer, Proc. Natl. Acad. Sci. USA 85 (1988) 8998–9002.
[9] P.D. Crowe, T.L. VanArsdale, B.N. Walter, C.F. Ware, C. Hession, B. Ehrenfels, J.L. Browning, W.S. Din, R.G. Goodwin, C.A. Smith, A lymphotoxin-β-specific receptor, Science 264 (1994) 707–710.
[10] J.L. Browning, I.D. Sizing, P. Lawton, P.R. Bourdon, P.D. Rennert, G.R. Majeau, C.M. Ambrose, C. Hession, K. Miatkowski, D.A. Griffiths, A. Ngam-ek, W. Meier, C.D. Benjamin, P.S. Hochman, Characterization of lymphotoxin-αβ complexes on the surface of mouse lymphocytes, J. Immunol. 159 (1997) 3288–3298.
[11] W.R. Force, B.N. Walter, C. Hession, R. Tizard, C.A. Kozak, J.L. Browning, C.F. Ware, Mouse lymphotoxin-β receptor. Molecular genetics, ligand binding, and expression, J. Immunol. 155 (1995) 5280–5288.
[12] A. Futterer, K. Mink, A. Luz, M.H. Kosco-Vilbois, K. Pfeffer, The lymphotoxin β receptor controls organogenesis and affinity maturation in peripheral lymphoid tissues, Immunity 9 (1998) 59–70.
[13] R.M. Locksley, N. Killeen, M.J. Lenardo, The TNF and TNF receptor superfamilies: integrating mammalian biology, Cell 104 (2001) 487–501.
[14] J.L. Browning, K. Miatkowski, I. Sizing, D. Griffiths, M. Zafari, C.D. Benjamin, W. Meier, F. Mackay, Signaling through the lymphotoxin β receptor induces the death of some adenocarcinoma tumor lines, J. Exp. Med. 183 (1996) 867–878.
[15] I.A. Rooney, K.D. Butrovich, A.A. Glass, S. Borboroglu, C.A. Benedict, J.C. Whitbeck, G.H. Cohen, R.J. Eisenberg, C.F. Ware, The lymphotoxin-β receptor is necessary and sufficient for LIGHT-mediated apoptosis of tumor cells, J. Biol. Chem. 275 (2000) 14307–14315.
[16] P. Yu, Y. Lee, W. Liu, R.K. Chin, J. Wang, Y. Wang, A. Schietinger, M. Philip, H. Schreiber, Y.X. Fu, Priming of naive T cells inside tumors leads to eradication of established tumors, Nat. Immunol. 5 (2004) 141–149.
[17] T. Hehlgans, B. Stoelcker, P. Stopfer, P. Muller, G. Cernaianu, M. Guba, M. Steinbauer, S.A. Nedospasov, K. Pfeffer, D.N. Mannel, Lymphotoxin-β receptor immune interaction promotes tumor growth by inducing angiogenesis, Cancer Res. 62 (2002) 4034–4040.

Experimental trial for diagnosis of pancreatic ductal carcinoma based on gene expression profiles of pancreatic ductal cells

Madoka Ishikawa,[1] Koji Yoshida,[2] Yoshihiro Yamashita,[1] Jun Ota,[1,3] Shuji Takada,[1] Hiroyuki Kisanuki,[1] Koji Koinuma,[1] Young Lim Choi,[1] Ruri Kaneda,[1] Toshiyasu Iwao,[4] Kiichi Tamada,[5] Kentaro Sugano[5] and Hiroyuki Mano[1,3,6]

[1]Division of Functional Genomics, Jichi Medical School, 3311-1 Yakushiji, Kawachi-gun, Tochigi 329-0498; [2]Department of Medicine, Kawasaki Medical School, Okayama 701-0192; [3]CREST, Japan Science and Technology Agency, 4-1-8, Honcho, Kawaguchi-shi, Saitama 332-0012; [4]Gastroenterological Center, Aizu Central Hospital, 1-1 Tsuruga-machi, Aizu-Wakamatsu, Fukushima 956-8611; and [5]Division of Gastroenterology, Jichi Medical School, 3311-1 Yakushiji, Kawachi-machi, Kawachi, Tochigi 329-0498, Japan

(Received November 18, 2004/Revised April 25, 2005/Accepted April 27, 2005/Online Publication July 22, 2005)

Pancreatic ductal carcinoma (PDC) remains one of the most intractable human malignancies, mainly because of the lack of sensitive detection methods. Although gene expression profiling by DNA microarray analysis is a promising tool for the development of such detection systems, a simple comparison of pancreatic tissues may yield misleading data that reflect only differences in cellular composition. To directly compare PDC cells with normal pancreatic ductal cells, we purified MUC1-positive epithelial cells from the pancreatic juices of 25 individuals with a normal pancreas and 24 patients with PDC. The gene expression profiles of these 49 specimens were determined with DNA microarrays containing >44 000 probe sets. Application of both Welch's analysis of variance and effect size-based selection to the expression data resulted in the identification of 21 probe sets corresponding to 20 genes whose expression was highly associated with clinical diagnosis. Furthermore, correspondence analysis and 3-D projection with these probe sets resulted in separation of the transcriptomes of pancreatic ductal cells into distinct but overlapping spaces corresponding to the two clinical classes. To establish an accurate transcriptome-based diagnosis system for PDC, we applied supervised class prediction algorithms to our large data set. With the expression profiles of only five predictor genes, the weighted vote method diagnosed the class of samples with an accuracy of 81.6%. Microarray analysis with purified pancreatic ductal cells has thus provided a basis for the development of a sensitive method for the detection of PDC. (*Cancer Sci* 2005; 96: 387–393)

Pancreatic ductal carcinoma (PDC), arising from the pancreatic ductal cells, accounts for more than 85% of all pancreatic malignancies, and is one of the most intractable malignancies in humans.[1,2] Effective therapy for PDC is hampered by the lack of specific clinical symptoms, with a 5-year survival rate of only 20 to 30%. An increase in the serum concentration of the protein CA19-9 is a reliable marker for PDC, but such an increase is only apparent in the advanced stages of disease.[3] Furthermore, although activating mutations of the *KRAS* oncogene have been detected in PDC cells, such mutations are also associated with other conditions, including chronic pancreatitis.[4,5]

DNA microarray analysis allows the simultaneous monitoring of the expression level of thousands of genes[6,7] and is therefore a potentially suitable approach for the identification of novel molecular markers for detection of the early stages of PDC. However, caution is warranted in simple comparisons between normal and cancerous pancreatic tissues. Because normal pancreatic tissue is composed mostly of exocrine and endocrine cells, and cancerous pancreatic tissue consists mostly of tumor cells that arise from ductal epithelial cells, a simple comparison between these two tissues tends to identify cell lineage-dependent gene expression differences.[8]

To minimize such misleading data that are attributable to population-shift effects, we have set up a depository for pancreatic ductal cells purified from pancreatic juice collected from patients during endoscopic retrograde cholangiopancreatography (ERCP). Comparison of such pancreatic ductal cell preparations between control individuals and PDC patients by DNA microarray analysis has the potential to identify specific gene markers for the latter. Indeed, an initial screening of a limited number of samples (from three individuals with a normal pancreas and six with PDC) with a DNA microarray of 3456 genes yielded candidates for new PDC marker genes.[8]

We have now expanded this project by using a larger number of specimens: 25 from individuals with a normal pancreas and 24 from PDC patients. Each purified preparation of pancreatic ductal cells was subjected to microarray experiments with Affymetrix HGU133 A&B GeneChips, which contain >44 000 probe sets corresponding to ~33 000 human genes. The application of sophisticated bioinformatics techniques to this large data set (a total of 2 156 000 data points) resulted in the establishment of an algorithm to differentiate transformed ductal cells from normal ones.

Materials and Methods

Preparation of pancreatic ductal cells. The study subjects comprised individuals who underwent ERCP and collection of pancreatic juice for cytological examination. The subjects gave informed consent and the study was approved by the institutional review board of Jichi Medical School. Diagnosis of patients was confirmed on the basis of the combination of results obtained by ERCP, cytological examination of pancreatic juice, abdominal computed tomography, and measurement of the serum concentration of CA19-9, as well as of follow-up observations. Approximately one-third of each specimen of pancreatic juice was used to purify MUC1$^+$ ductal cells.[9]

Cells were collected from the pancreatic juice by centrifugation and were resuspended in 1 mL of MACS binding buffer (150 mM NaCl, 20 mM sodium phosphate [pH 7.4], 3% fetal bovine serum, 2 mM ethylenediamine tetraacetic acid). They were then incubated for 30 min at 4°C with 0.5 μg of a mouse

[6]To whom correspondence should be addressed. E-mail: hmano@jichi.ac.jp

Abbreviations: ACTB, β-actin; EPPK1, epiplakin 1; ERCP, endoscopic retrograde cholangiopancreatography; H2BFB, H2B histone family, member B; KNN, *k* nearest neighbor; NRCAM, neuronal cell adhesion molecule; PCR, polymerase chain reaction; PDC, pancreatic ductal carcinoma; PLOD2, procollagen-lysine, 2-oxoglutarate 5-dioxygenase 2; RASAL2, RAS protein activator-like 2; SCGB3A1, secretoglobin, family 3A, member 1; SST, somatostatin; WV, weighted vote.

© Japanese Cancer Association doi:10.1111/j.1349-7006.2005.00064.x

monoclonal antibody to MUC1 (Novocastra Laboratories, Newcastle upon Tyne, UK), washed with MACS binding buffer, and mixed with MACS MicroBeads conjugated with antibodies to mouse immunoglobulin G (Miltenyi Biotec, Auburn, CA, USA). The resulting mixture was subjected to chromatography on a miniMACS magnetic cell separation column (Miltenyi Biotec), and the eluted MUC1$^+$ cells were divided into portions and stored at −80°C. Portions of the unfractionated cells as well as the isolated MUC1$^+$ cells of each individual were stained with Wright–Giemsa solution to examine the purity of the ductal cell-enriched fractions.

Microarray experiments. Total RNA was extracted from the MUC1$^+$ cell preparations with the use of an RNeasy Mini column and RNase-free DNase (Qiagen, Valencia, CA, USA) and was subjected to two rounds of mRNA amplification with T7 RNA polymerase.[10] The high fidelity of the amplification step has been demonstrated previously.[11] One microgram of the amplified cRNA was then converted to double-stranded cDNA by PowerScript reverse transcriptase (BD Biosciences Clontech, Palo Alto, CA, USA), and the cDNA was used to prepare biotin-labeled cRNA with an ENZO BioArray Transcript Labeling Kit (Affymetrix, Santa Clara, CA, USA). Hybridization of the labeled cRNA with GeneChip HGU133 A&B microarrays, which contain >44 000 probe sets, was performed with the GeneChip system (Affymetrix). The mean expression intensity of the internal positive control probe sets[12] was set to 500 arbitrary units (U) in each hybridization, and the fluorescence intensity of each test gene was normalized accordingly. All normalized array data are available at the Gene Expression Omnibus web site (http://www.ncbi.nlm.nih.gov/geo) under the accession number GSE1542.

Statistical analysis. Hierarchical clustering of the data set, Welch's analysis of variance (ANOVA), and k nearest neighbor (KNN) method-based class prediction were performed with GeneSpring 6.2 software (Silicon Genetics, Redwood, CA). The weighted vote (WV) method[13] was performed with GeneCluster 2.1.7.[14] Correspondence analysis[15] for all genes showing a significant difference in expression was performed by using ViSta software.[16] Each sample was plotted in three dimensions based on the coordinates obtained from the correspondence analysis. With the exception of the effect-size selection, in which linear values were used for calculation, all normalized expression values were transformed to logarithms prior to analyses.

Real-time PCR analysis. Portions of nonamplified cDNA were subjected to PCR with a QuantiTect SYBR Green PCR Kit (Qiagen). The amplification protocol comprised incubations at 94°C for 15 s, 57°C for 30 s, and 72°C for 60 s. Incorporation of the SYBR Green dye into PCR products was monitored in real time with an ABI PRISM 7900 HT sequence detection system (PE Applied Biosystems, Foster City, CA, USA), thereby allowing determination of the threshold cycle (C_T) at which exponential amplification of products begins. The C_T values for cDNA corresponding to the β-actin gene (*ACTB*) and to the target genes were used to calculate the abundance of target gene mRNA relative to that of *ACTB* mRNA. The oligonucleotide primers for PCR were as follows: 5′-CCATCATGAAGTGTGACGTGG-3′ and 5′-GTCCGCCTAGAAGCATTTGCG-3′ for *ACTB*, 5′-CCCGTGAACCACCTCATAG-3′ and 5′-AGCGTCTTGTCCTCAGGTGTA-3′ for the secretoglobin, family 3A, member 1 gene (*SCGB3A1*), and 5′-GATGAAATGAGGCTTGAGCTG-3′ and 5′-GTTTCTAATGCAAGGGTCTCG-3′ for the somatostatin gene (*SST*).

Results

Transcriptome of pancreatic ductal cells. As demonstrated previously, affinity purification with antibodies to MUC1 yielded an apparently homogeneous preparation of pancreatic ductal cells.[8] With this approach, we purified pancreatic ductal cell specimens from 25 individuals with a normal pancreas and 24 patients with PDC. Clinical characteristics for the latter individuals are summarized in Table 1. All 49 specimens were each subjected to DNA microarray analysis with Affymetrix HGU133 A&B GeneChips, which contain >44 000 probe sets.

Table 1. Clinical characteristics of patients with PDC

Patient	Age (years)	Sex	Cytological examination	Atypical cell proportion*	Clinical stage†
ID073	74	Male	V	H	IVa
ID086	72	Female	IV	M	IVa
ID088	65	Male	V	L	IVb
ID089	70	Female	III	L	III
ID090	72	Male	III	L	IVa
ID095	85	Female	III	L	0
ID096	76	Female	IV	L	IVa
ID098	61	Female	IV	L	IVa
ID103	65	Male	V	H	IVb
ID117	76	Female	IV	L	IVa
ID119	73	Female	V	L	IVa
ID120	70	Female	III	M	0
ID125	75	Male	II	L	I
ID131	67	Female	II	L	IVa
ID142	69	Male	III	H	I
ID147	51	Male	V	L	IVb
ID202	56	Female	III	M	IVa
ID203	73	Male	III	M	I
ID218	51	Male	III	L	0
ID224	71	Male	V	L	IVa
ID225	50	Female	III	L	IVa
ID227	65	Male	I	L	III
ID229	60	Female	IV	M	IVa
ID234	71	Male	III	L	IVa

*Isolated ductal cells contained <20% (L), 20–40% (M) or ≧ 40% (H) of atypical cells. †Clinical stage was determined according to the proposal of Isaji *et al.*[25]

For analysis of the gene expression data, we first set the condition that the expression level of a given probe set should receive the 'Present call' (from Microarray Suite 5.0 software) in at least 30% ($n = 15$) of the samples in order to exclude transcriptionally silent genes from the analysis. A total of 7778 probe sets fulfilled this selection criterion. Unsupervised two-way hierarchical clustering analysis[17] was then applied to the 49 specimens based on the expression profiles of these 7778 probe sets, generating a dendrogram in which the samples are clustered according to the similarity in expression pattern of the probe sets (Fig. 1). Although this dendrogram contained a large branch consisting mostly of PDC patients, normal and cancer specimens did not form separate, diagnosis-dependent branches. The transcriptome of virtually all expressed genes thus did not differ sufficiently between normal and cancerous ductal cells to allow diagnosis.

PDC-specific molecular signature. To capture a PDC-specific molecular signature, we next identified genes whose expression level differed significantly between the normal and cancerous ductal cells. Application of Welch's ANOVA ($P < 0.001$) for this purpose yielded 26 out of the 7778 probe sets examined. However, some of the probe sets thus identified had low absolute expression levels throughout the samples, even though the ratio of the expression levels between the two classes was relatively large. To eliminate such 'nearly silent' genes and to enrich genes whose expression level was markedly increased in at least one of the classes, we further selected those whose effect size (absolute difference in mean expression intensities)[18] between the two classes was ≧ 50 U.

© Japanese Cancer Association doi:10.1111/j.1349-7006.2005.00064.x

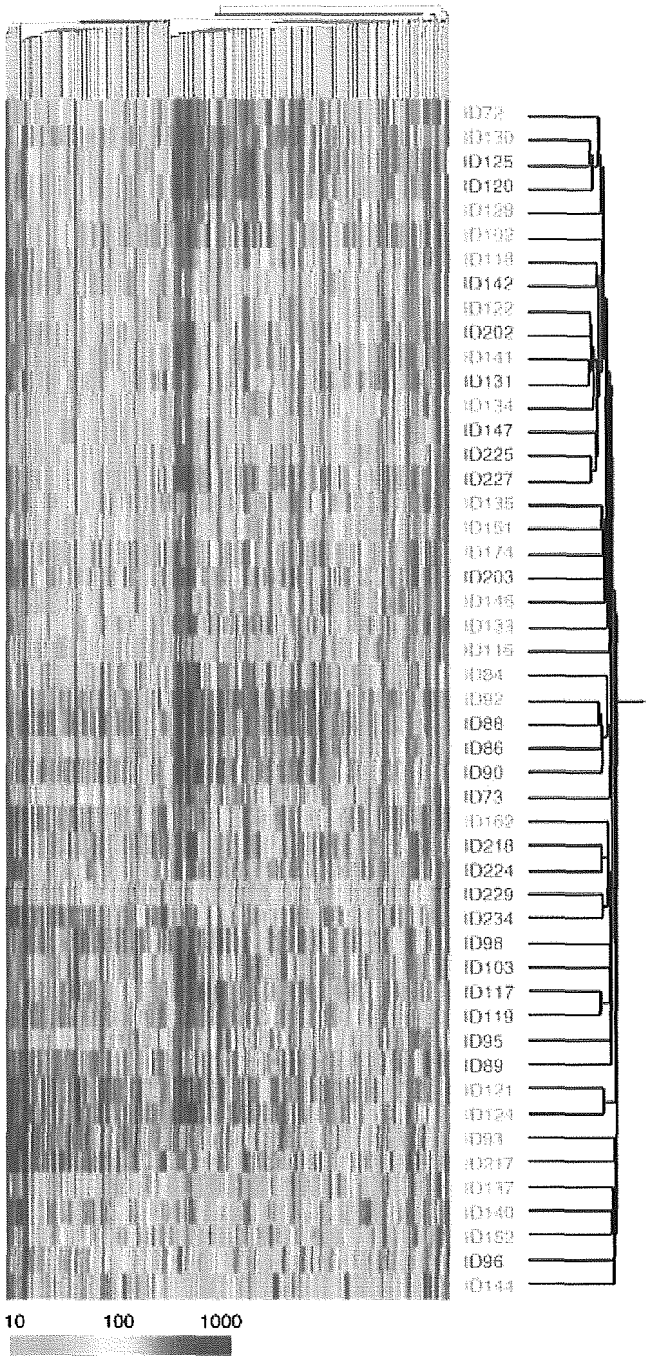

Fig. 1. Gene expression profiles of the purified pancreatic ductal cells. Hierarchical two-way clustering of the study subjects (normal ductal cell specimens [green] and PDC specimens [red]) was performed on the basis of the expression profiles of 7778 probe sets. Each column corresponds to a single probe set, and each row corresponds to a separate subject. The expression level of probe sets is color-coded according to the indicated scale.

With this approach, we identified 21 probe sets (corresponding to 20 independent genes) whose expression levels differed significantly between the two clinical conditions. Construction of a dendrogram for the expression profiles of these 21 probe sets revealed that the subjects were grouped into two major branches (Fig. 2a). Although each branch corresponded approximately to the two clinical classes, a few subjects were still misclassified in both branches. It was not clear, however, whether this failure to clearly separate the two clinical classes was due to an inadequacy of the separation power of the clustering method or to the heterogeneity of the samples within each clinical class. Furthermore, these results did not address whether normal and cancerous ductal cells are truly distinct from each other from the point of view of gene expression profiles.

To address these issues, we attempted to visualize the similarity or difference between the two classes. Correspondence analysis is a relatively new approach to the decomposition of multidimensional data.[15] It allows not only a low-dimensional projection of expression profiles for numerous genes, but also measurement both of the contribution of each gene to a given extracted dimension and of the contribution of each extracted dimension to the total complexity. Correspondence analysis of the expression data of the 21 probe sets shown in Fig. 2a reduced the number of dimensions from 21 to three. On the basis of the calculated 3-D coordinates for each sample, the specimens were then projected into a virtual space (Fig. 2b). Although most of the normal samples were positioned in a region of the space distant from that occupied by the PDC specimens, the two groups were not separated completely. Decomposition of the data set was thus not sufficiently effective to achieve a high accuracy in differential diagnosis.

Supervised class prediction. We next attempted class prediction by using two supervised algorithms. The WV method was recently developed to assign binary classes based on gene expression profiles.[13] A defined number of 'class predictor' genes whose expression contrasts the two classes most effectively are first selected in a training data set. A weighting factor, which reflects how well a gene is correlated with the class distinction, is also calculated for each gene. The expression levels of the class predictors are then quantitated in the test data set, and the 'prediction strength' is determined on the basis of the expression intensities and weighting factors of the predictors. The WV method has been successfully used to differentiate acute myeloid leukemia from acute lymphoid leukemia,[13] as well as diffuse large B cell lymphoma with poor prognosis from that with good prognosis.[19]

The KNN method, like the WV method, first involves the selection of a defined number of predictor genes. It then finds nearest neighbors to the classes based on a distance function for pairs of observations. The KNN method predicts the class of a given test sample based on the majority of votes among the nearest neighbors.[20]

To measure precisely the class prediction ability of these two methods, we performed a cross-validation trial for each with our data set: One sample was therefore set aside and the program was trained with the remaining 48 samples; the class of the withheld test sample was then predicted by the program, and the trial was repeated for each of the 49 samples to calculate the overall accuracy of the program.

For both WV and KNN methods, the cross-validation was performed with the 49 specimens and with different numbers of class predictor genes (n = 1 to 20, 30, 40, 50, 60, 70, 80, 90, or 100). Both methods had similar error rates, with the WV method having a slightly lower error rate than the KNN method (Fig. 3a). The best prediction accuracy (81.6%) was obtained by the WV method with five class predictor genes. In this cross-validation, different sets of five predictors were selected for each leave-one-out trial, with a total of 11 probe sets (corresponding to 10 genes) used as predictors. Two-way clustering of the expression profiles of these 11 probe sets yielded the dendrogram shown in Fig. 3b. It should be noted that two probe sets (DKFZp564I1922 and EPPK1) were selected as the predictors in all 49 leave-one-out trials.

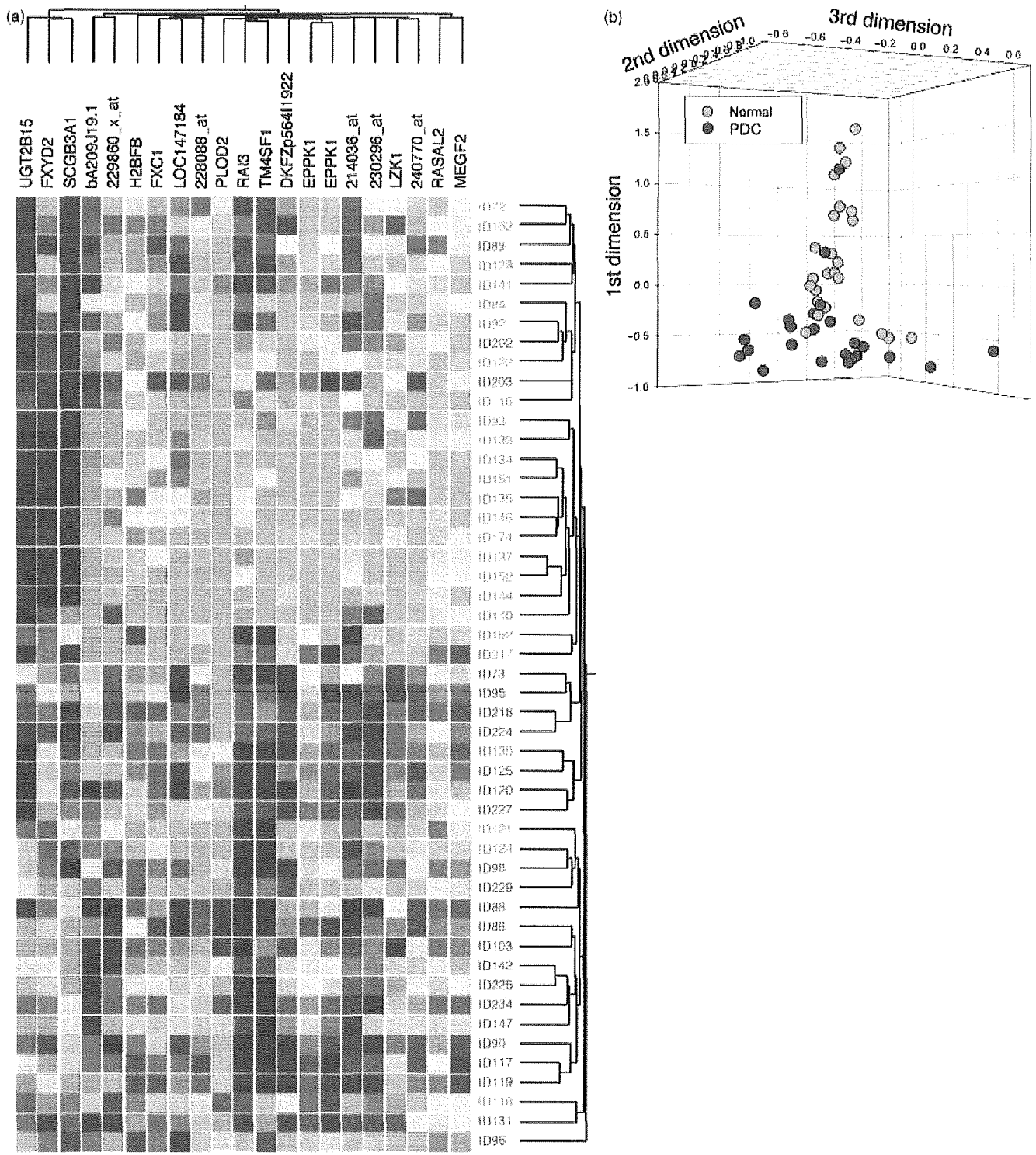

Fig. 2. Isolation of a PDC-specific molecular signature. (a) Dendrogram of the 21 probe sets whose expression level differed significantly (Welch's ANOVA, $P < 0.001$) with an effect size of ≧ 50 U between normal and cancerous specimens. Each row corresponds to a separate subject, and each column to a probe set whose expression is color-coded according to the scale in 1. Gene symbols are shown at the top; 229860_x_at, 228088_at, 214036_at, 230296_at, and 240770_at are expressed sequence tag IDs designated by Affymetrix. Detailed information on the genes and their expression levels is provided in Supplementary Information at the *Cancer Science* web site. (b) Correspondence analysis of the 21 probe sets identified three major dimensions in their expression profiles. Projection of the specimens into a virtual space with these three dimensions revealed that those from individuals with a normal pancreas and those from patients with PDC were partially separated.

© Japanese Cancer Association doi:10.1111/j.1349-7006.2005.00064.x

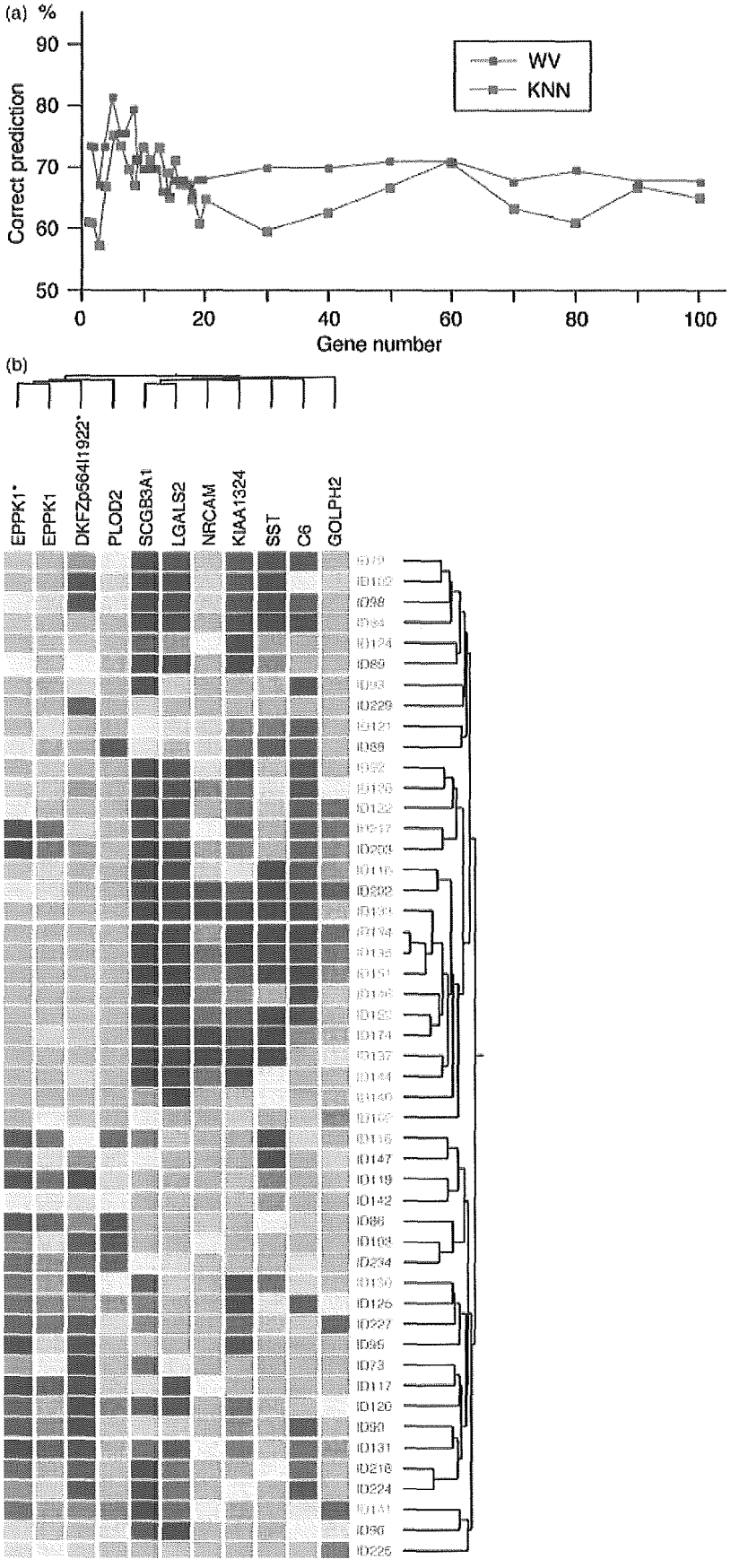

Fig. 3. Supervised class prediction. (a) Cross-validation trials for class prediction of normal or PDC specimens based on various numbers of predictor genes were performed with the WV or KNN methods. Correct prediction rate (%) is plotted for each trial. (b) Expression profiles of 11 probe sets identified by the WV method with five predictors. Samples are clustered according to the similarity in the expression pattern of the 11 probe sets. Asterisks indicate the two probe sets selected in all trials. Detailed information on the genes and their expression levels is provided in Supplementary Information at the *Cancer Science* web site.

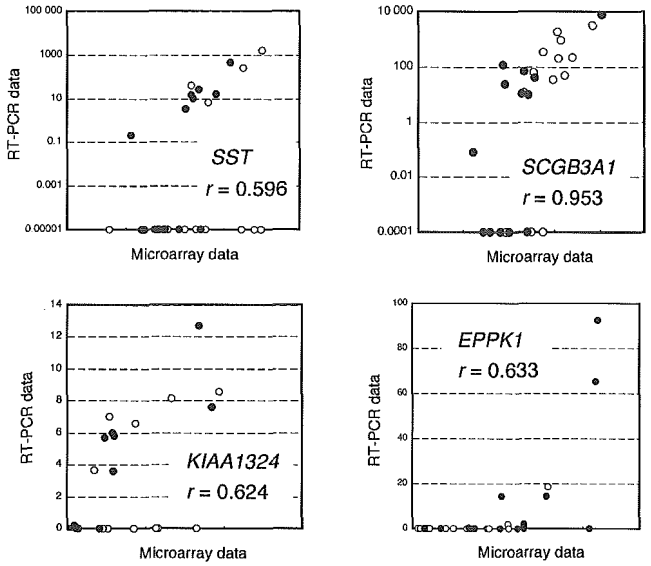

Fig. 4. Validation by reverse transcription and real-time PCR analysis of gene expression profiles obtained by microarray analysis. The relative amounts of mRNA corresponding to *SST, SCGB3A1, KIAA1324* or *EPPK1* in the MUC1$^+$ cells derived from (○) healthy individuals or (●) patients with PDC were determined by reverse transcription and real-time PCR with *ACTB* transcripts as the internal standard. The resulting values are plotted against those obtained by microarray analysis. Pearson's correlation coefficient (*r*) values are provided for each comparison.

Confirmation of expression data. To confirm the gene expression profiles obtained by microarray analysis, we measured the mRNA levels of some genes by reverse transcription and quantitative real-time PCR analysis. The relative amounts of mRNA derived from the *SST* (GenBank accession number NM_001048) or *SCGB3A1* (GenBank accession number AA742697) genes, for example, determined by this latter approach were highly correlated with those quantitated by microarray analysis (Fig. 4).

Discussion

In the present study, we constructed the largest gene expression database available to date for pancreatic ductal cells. Our statistical approach to identify genes associated with a diagnosis of PDC resulted in the extraction of 21 probe sets, three of which were preferentially expressed in normal ductal cells and the remaining 18 were preferentially expressed in cancerous ductal cells. The latter group contained the genes for H2B histone family member B (*H2BFB*; GenBank accession number BC002842), RAS protein activator-like 2 (*RASAL2*; GenBank accession number NM_004841), procollagen-lysine, 2-oxoglutarate 5-dioxygenase 2 (*PLOD2*; GenBank accession number NM_000935), adlican (DKFZp564I1922; GenBank accession number AF245505), and epiplakin 1 (*EPPK1*; GenBank accession number AL137725). H2BFB functions as a linker histone in nucleosome compaction.[21] The increased expression of *H2BFB* in PDC cells therefore probably reflects the increased proliferation rate of these cells. RASAL2 shares a GTPase-activating protein (GAP)-related domain with members of the RAS-GAP family of proteins and is thought to contribute to the regulation of small GTP-binding proteins. *RASAL2* is localized within the prostate cancer susceptibility locus at chromosome 1q25[22], so an altered activity of the encoded protein might thus be directly linked to carcinogenesis.

The expression profile of these disease-associated genes was not, however, sufficient to separate the specimens into the normal or cancer class with a high accuracy. We therefore applied sophisticated algorithms in the supervised mode in an attempt to achieve this goal. In our trials of the WV and KNN methods with various numbers of predictor genes, the WV method trained with five genes gave the best result. The accuracy of correct diagnosis achieved (81.6%) is higher than that obtained by cytological examination of pancreatic juice.[23]

In the 'leave-one-out' trials for all 49 samples, a total of 11 probe sets were chosen by the WV algorithm as the class predictors. These probe sets corresponded to 10 genes, including those for EPPK1, DKFZp564I1922, PLOD2, SCGB3A1, SST, and neuronal cell adhesion molecule (*NRCAM*; GenBank accession number NM_005010). NRCAM belongs to the immunoglobulin (Ig) superfamily of proteins, contains multiple repeats of the Ig domain in its extracellular region, and is expressed at the surface of neuronal cells. The DKFZp564I1922 protein also contains 12 repeats of the Ig domain.[24] Increased expression of these Ig domain-containing proteins may thus be a specific property and a novel molecular marker of PDC.

Among the 10 genes used in the WV analysis, only two (those for EPPK1 and DKFZp564I1922) were chosen as predictors in all 49 trials. In addition, the Welch's ANOVA strategy and the WV method selected five probe sets in common, including two sets for EPPK1, one for SCGB3A1, one for PLOD2, and one for DKFZp564I1922.

Cytological examination revealed that, among the individuals with PDC in our study, 16 patients had <20% of atypical cells in the purified ductal cell specimens ('L' in Table 1), three patients had ≧ 40% of such cells ('H'), and the other five patients had 20–40% of such cells ('M'). We thus examined whether the proportion of atypical cells in the specimens affected the expression intensities of the selected genes. The expression levels of the genes in Fig. 2a was, for instance, compared by Student's *t*-test between the individuals in the L and M groups, and between those in the M and H groups. Surprisingly, none of the genes in Fig. 2a were differentially expressed in a significant manner between these groups (data not shown). Therefore, our microarray-based prediction scheme should be of clinical importance even for patients with pancreatic juice containing small amounts of cancer cells.

Our strategy to identify a PDC-specific gene expression profile for purified pancreatic ductal cells should provide the basis for several possible scenarios for the early detection of PDC in the clinical setting. One scenario would be a microarray-based diagnosis of PDC with a sophisticated algorithm for analysis of the expression of a limited number of genes (as demonstrated in the present study). A second scenario would require an extension of our project to isolate single gene markers specific to PDC; the expression of such genes should be negligible in non-cancerous cells but would be markedly increased in cancerous cells. Such PDC-specific single gene markers would be good candidates for the construction of a sensitive PCR-based detection system for PDC. A third scenario may involve the identification of soluble proteins among the products of PDC-specific genes that could be detected in the serum of patients. Further expansion of our gene expression database would probably facilitate the development of such detection systems for PDC, which would improve the long-term prognosis of individuals with this intractable disease.

Acknowledgments

This work was supported in part by a Grant-in-Aid for research on the Third Term Comprehensive Control Research for Cancer from the Ministry of Health, Labour, and Welfare of Japan, and by a grant from the Research Foundation for Community Medicine.

© Japanese Cancer Association doi:10.1111/j.1349-7006.2005.00064.x